Approximation of Inertial Measurement Unit Data to Time Series Kinematic Data Through Correlation Analysis and Machine Learning

William Fröhlich[1][a], Rafael Bittencourt[1], Sandro Rigo[2][b], Rafael Baptista[1][c] and César Marcon[1][d]

[1]*School of Technology, Pontifical Catholic University of Rio Grande do Sul (PUCRS), Porto Alegre, Brazil*

[2]*Universidade do Vale do Rio dos Sinos (UNISINOS), São Leopoldo, Brazil*

Keywords: Gait Analysis, Inertial Measurement Units, Kinematic, Machine Learning, Correlation.

Abstract: Accurate results are traditionally obtained in gait analysis using gold-standard methods such as motion capture with kinematic cameras and force platforms in biomechanics labs. However, these techniques are expensive, time-consuming, and require controlled environments, limiting their accessibility for more clinical and research applications. This study explores the potential of inertial measurement units as a cost-effective alternative. We focused on extracting features from Inertial Measurement Unit (IMU) data, such as acceleration and angular velocity, and derived metrics like speed and angular acceleration to approximate the accuracy of kinematic camera data. Following extensive preprocessing of inertial and kinematic datasets, we applied analytical methods, including Pearson correlation and cross-correlation, to identify significant relationships between the two data sources. We employed the most strongly correlated features to train Machine Learning models, Clustering techniques to assess the consistency and reliability of the results, and the Random Forest algorithm to train and evaluate the models' capacity for time series prediction. Our findings suggest that certain aspects of IMU data strongly correlate with kinematic outcomes. This indicates that IMUs can replicate results traditionally obtained through more complex and costly methods under specific conditions.

1 INTRODUCTION

Gait analysis is a critical tool for diagnosing neurodegenerative diseases, optimizing athletic performance, and understanding the broader implications of gait on health and lifestyle. Traditionally, motion capture systems using kinematic cameras and plantar pressure measurements have been the gold standard for precise gait analysis due to their accuracy and ability to capture detailed biomechanical data (Zhang et al., 2017) (Jakob et al., 2021). However, these methods come with significant limitations, such as being expensive, requiring specialized equipment, and being performed in controlled laboratory environments, restricting their accessibility in clinical and research settings (Benson et al., 2018).

In response to these challenges, Inertial Measurement Units (IMUs) have emerged as a promising alternative. IMUs are portable, cost-effective, and versatile, allowing for gait analysis outside traditional lab settings (Akhtaruzzaman et al., 2016) (Kotiadis et al., 2010). Despite their potential, the data collected by IMUs must be validated against gold-standard methods like optical motion capture to ensure accuracy and reliability (Kvist et al., 2024). This validation is essential for IMUs to be considered viable substitutes or complements of established technologies.

Biomechanics and gait assessments are fundamental for identifying locomotor issues, playing a crucial role in personalized rehabilitation and athletic performance enhancement (Benson et al., 2018) (Akhtaruzzaman et al., 2016). Wearable devices, especially IMUs, have gained attention due to their convenience and ability to capture gait data in real-world environments. However, the challenge remains in ensuring that the data obtained from wearables can achieve the precision of traditional motion capture labs (Kvist et al., 2024).

Motion capture systems with high-precision cameras and force platforms provide high accuracy, capturing joint angles, stride length, speed, and muscle activity. In contrast, wearable sensors lack the accuracy of lab-based methods, but they are versatile and can record real-time data continuously (Kotiadis et al., 2010). We compare these approaches, exploring their current applications and identifying the research gaps related to wearable IMU and kinematic data integration.

[a] https://orcid.org/0000-0003-3551-2623
[b] https://orcid.org/0000-0001-8140-5621
[c] https://orcid.org/0000-0003-1937-6393
[d] https://orcid.org/0000-0002-7811-7896

Fröhlich, W., Bittencourt, R., Rigo, S., Baptista, R. and Marcon, C.
Approximation of Inertial Measurement Unit Data to Time Series Kinematic Data Through Correlation Analysis and Machine Learning.
DOI: 10.5220/0013115800003911

In *Proceedings of the 18th International Joint Conference on Biomedical Engineering Systems and Technologies (BIOSTEC 2025) - Volume 2: HEALTHINF*, pages 75-86
ISBN: 978-989-758-731-3; ISSN: 2184-4305

One of the leading research challenges is correlating IMU data with kinematic data obtained from motion capture systems (Silva and Stergiou, 2020). A strong correlation would validate IMUs as reliable tools for capturing gait metrics, making them suitable for broader applications. Artificial intelligence (AI) and Machine Learning (ML) are particularly well-suited for this task, as they can process large datasets, uncover complex patterns, and model relationships between inertial and kinematic data (Silva and Stergiou, 2020) (Benson et al., 2018).

This study investigates how IMU data, such as acceleration, gyroscope, roll, and yaw, correlate with camera kinematic data. We applied Pearson correlation and cross-correlation techniques to identify significant relationships between the two datasets. Based on these correlations, we developed Machine Learning models to predict kinematic parameters using IMU data. The subsequent validation of these models and cluster analysis offers valuable insights into the feasibility of using IMUs as complementary or alternative tools to traditional motion capture.

Using these correlations as a foundation, we developed ML models, including Random Forest (RF) and Linear Regression (LR), to predict kinematic parameters from IMU data. This approach leverages the capacity of AI and ML to process large datasets and uncover complex, nonlinear relationships between wearable sensor data and biomechanical measurements (Silva and Stergiou, 2020) (Benson et al., 2018). In summary, wearable IMUs offer significant advantages in terms of flexibility and real-world applicability, but achieving the same level of precision as traditional motion capture is still a challenge. By integrating AI-driven models, we provide a step forward in bridging the gap between IMU and kinematic data.

2 RELATED WORK

Biomechanics and gait assessment are essential tools for identifying locomotion problems, with significant impact across various fields, including personalized rehabilitation strategies and athletic performance enhancement (Benson et al., 2018) (Akhtaruzzaman et al., 2016). Understanding human biomechanics can improve health outcomes, refine athletic abilities, and accelerate recovery processes (Silva and Stergiou, 2020). In recent years, wearable devices for gait analysis have gained popularity due to their portability and ease of use, allowing gait analysis outside traditional biomechanics labs (Benson et al., 2018). However, it is crucial to validate wearable data using gold-standard methods to ensure accuracy and precision (Kvist et al., 2024).

Biomechanics laboratories, equipped with high-speed cameras, force platforms, and electromyographs, capture detailed movement data during walking (Akhtaruzzaman et al., 2016). These labs offer precise information on joint angles, stride length, speed, and muscle activity, making them the gold standard for gait analysis (Jakob et al., 2021) (Zhang et al., 2017). On the other hand, wearable sensors provide a more versatile alternative, although they generally do not achieve the same level of accuracy and precision (Akhtaruzzaman et al., 2016). These devices typically consist of inertial sensors placed on key body areas, recording real-time movement without environmental restrictions (Kotiadis et al., 2010).

Despite the advantages of wearables, a research gap exists in correlating data from inertial sensors with data from biomechanics labs that use optical cameras for motion capture (Zhou et al., 2020) (Tsakanikas et al., 2023) (Silva and Stergiou, 2020). Many studies focus on specific diagnoses, like Parkinson's disease detection, rather than directly comparing the datasets (Borzì et al., 2023) (da Rosa Tavares et al., 2023). Correlation analysis is crucial to assess how well kinematic data matches inertial data (Desai et al., 2024) (He et al., 2024) (Kvist et al., 2024) (Ripic et al., 2023) (Rousanoglou et al., 2024). Still, preprocessing steps, such as filtering and data normalization, are needed before analysis. Furthermore, clustering techniques could enhance data grouping and identification using artificial intelligence (Caldas et al., 2020) (Kim et al., 2022) (Nguyen et al., 2019).

This study aims to explore the differences between motion capture labs and wearable sensors and to evaluate state-of-the-art applications of both tools in gait analysis. Specifically, it seeks to identify research gaps related to correlating kinematic and inertial data, potentially contributing to establishing a gold-standard approach using inertial data alone.

3 METHODOLOGY

Figure 1 shows the methodology used to evaluate the similarities and correlations between kinematic gait data obtained from gold-standard motion capture systems and inertial data collected from wearable sensors. The process begins with data collection (Subsection 3.1) in a biomechanics laboratory equipped with high-speed cameras and a wearable IMU system. After collecting the data, we conducted experiments to determine the optimal preprocessing steps, drawing from state-of-the-art approaches, as discussed in Subsection 3.2. Next, we applied correlation algorithms to analyze the relationships and similarities between the kinematic and inertial data (Subsection 3.3). Based on these correlation results, we used AI algorithms to perform cluster analysis (Subsection 3.5), focusing on the three phases of gait: double stances and single stances with the left and right feet. Finally, we conducted exploratory Machine Learning experiments (Subsection 3.6) using RF and Linear Regression algorithms. These stages formed the basis for training models to evaluate how well inertial data can capture gait patterns compared to the gold-standard kinematic data and evaluate the feature importance in each model of the kinematic points.

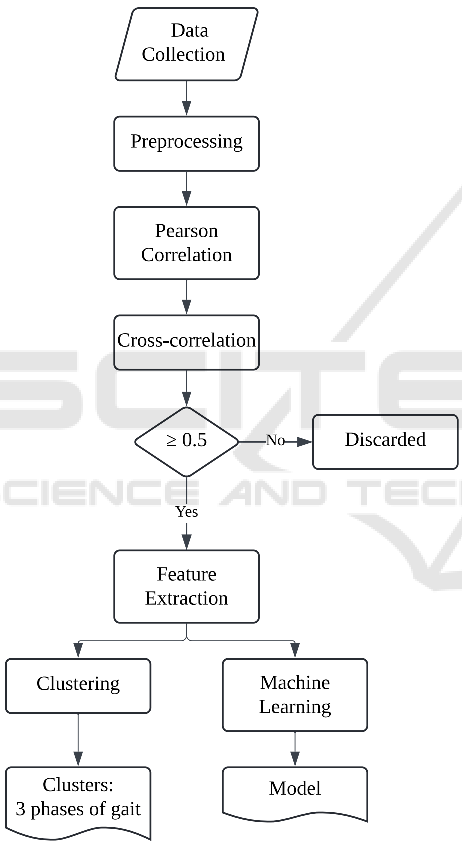

Figure 1: Flowchart for evaluating similarities and correlation between kinematic and inertial data.

3.1 Data Collection

The data collection experiments had the ethics committee's approval and followed a standardized gait analysis protocol, where participants walked along a straight path, stepped over a force platform, and then returned. The procedure was conducted using the equipment from the GaitLab biomechanics laboratory (BTS Bioengineering, 2024b), which includes motion capture cameras and a force platform. The wearable sensor used in the experiments was the GWalk (BTS Bioengineering, 2024a), a device positioned on the participants' lumbar region that collects inertial data from accelerometers and gyroscopes, including acceleration (*acc*) and rotational motion (*gyro*), both on three axes, and roll (*roll*), pitch (*pitch*), and yaw (*yaw*) orientation angles. Figure 2 illustrates the placement of the wearable IMUs on the participants during data collection. It also shows the orientation of the data relative to the X, Y, and Z axes and the direction of data rotation. The raw data were extracted from the computers using software to collect data from the devices.

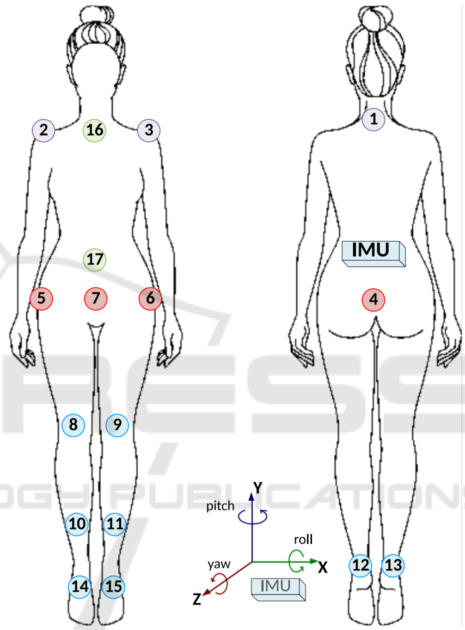

Figure 2: Placement of kinematic points and wearable IMUs for the data collection experiments.

The data from the biomechanics laboratory include many kinematic points, but to make the study more efficient and focused, we have selected the key points based on the state of the art (Delval et al., 2021). We categorized these points into groups, according to point in Figure 2: for the Upper Trunk, we selected the C7 cervical vertebra (*c7* - 1), right shoulder (*r_should* - 2), and left shoulder (*l_should* - 3); for the Lower Trunk, we chose the sacrum (*sacrum_s* - 4), right anterior superior iliac crest (*r_asis* - 5), left anterior superior iliac crest (*l_asis* - 6), and the midpoint between the iliac crests (*MIDASIS* - 7). For the legs, the selected points are the right (*r_knee_1* - 8) and left knee (*l_knee_1* - 9), right (*r_mall* - 10) and left ankle (*l_mall* - 11), right (*r_heel* - 12), and left heel (*l_heel* - 13), and right (*r_met* - 14) and left metatarsal (*l_met* - 15). Two additional valuable points are the average shoulder position (PO - 16) and the center of mass (SHO - 17). In the collected kinematic data, as shown in Figure 2, the X-axis represents lateral movement, the Y-axis represents upward movement, and the Z-axis represents forward walking movement. In addition to the inertial data, force platforms provide measurements for both feet (r_force and l_force) along three axes. The collected dataset[5] is available for reproduction

3.2 Data Preprocessing

In gait analysis, abrupt changes along the X, Y, and Z axes, particularly derived from acceleration data, represent the rate of change of acceleration over time. This information is vital as it highlights sudden shifts in the forces acting on the body, which may indicate specific gait events or irregularities.

We developed data processing and analysis routines using Python 3.10, employing libraries such as NumPy, Pandas, Scipy, and Scikit-Learn. Data preprocessing is crucial in ensuring the data is clean, consistent, and ready for advanced analysis. The preprocessing workflow incorporated multiple steps, all guided by the latest methodologies in gait analysis and supported by relevant research (Millecamps et al., 2015), (Burdack et al., 2020), (Parashar et al., 2023).

After loading the data, the first step addressed data issues, often represented as "Not a Number" (NaN), which can arise from various reasons. Proper handling of NaNs is crucial, as they can skew results or degrade model performance if left unaddressed. Initially, we removed NaNs from the start and end of the files, where the absence of data likely corresponded to periods outside the recorded movement. Next, we conducted experiments by imputing NaNs with the mean of surrounding values to fill in the gaps. However, in cases where data was missing due to specific conditions, such as during the swing phase when the force platforms might not detect force, we replaced NaNs with zeros, indicating the absence of foot contact with the platform. After experimenting with these imputation methods, the optimal solution was replacing missing data caused by a technical failure with the mean of the surrounding data and imputing zeros for data not captured by the force platforms. This strategy ensured that the data remained as accurate and unbiased as possible for further analysis.

We applied interpolation techniques to address gaps further. Linear interpolation, in particular, estimated missing values based on neighboring data points. This approach assumes a smooth transition between known values, making it ideal for time series data like gait measurements, where maintaining continuity is crucial for accurate analysis.

Next, we filtered the data to reduce the noise of the signal. We tested with Butterworth filters, including low-pass, band-pass, and high-pass configurations. The low-pass Butterworth filter proved the most effective, eliminating high-frequency noise while preserving crucial patterns in the sensor data. For both the GaitLab data sampled at 250 Hz and the GWalk data sampled at 100 Hz, we applied a 3.0 Hz cutoff frequency with a 5th-order filter. This low-pass filter was particularly advantageous, as it retained the essential low-frequency components critical for gait analysis.

Following noise reduction, we normalized the data, ensuring that all features were on the same scale, preventing any single feature from dominating the analysis. We tested standardization, which adjusts data to have a mean of zero and a standard deviation of one, and Min-Max scaling, which rescales data to a fixed range. Min-Max scaling yielded better results, particularly for datasets with features on different scales, by preserving the relative importance of each feature while ensuring uniform analysis.

The final preprocessing step was data merging, an essential task given the equipment's differing sampling rates, such as 250 Hz for GaitLab and 100 Hz for GWalk. Temporal alignment of the datasets is necessary to ensure accurate comparison and integration. This was accomplished by merging the data based on precise timestamps from each system, allowing for synchronized analysis of the gait cycles captured by both kinematic cameras and inertial sensors.

Through these comprehensive preprocessing steps, we ensured the data was of high quality, accurately reflecting the subjects' movements, and ready for the following stages of correlation analysis and ML model development.

3.3 Data Correlations

The correlation analysis between kinematic, force, and inertial data is crucial for identifying similarities and relationships between these datasets. This analysis is the foundation for validating whether IMUs can effectively replicate the results traditionally obtained through more complex and expensive methods. In this study, we employed Pearson correlation (Section 3.3.1 and cross-correlation (Section 3.3.2 techniques to assess the degree of similarity between the data from these different sources. Based on the strongest relationships between IMU and kinematic points, we will move forward using AI techniques.

[5] www.kaggle.com/datasets/wrfrohlich/artemis-dataset

3.3.1 Pearson Correlation Analysis

Pearson correlation evaluates the strength and direction of the linear relationship between two quantitative variables. The Pearson correlation coefficient ranges from -1 to 1. A value of -1 indicates a perfect negative correlation, 0 indicates no correlation, and 1 indicates a perfect positive correlation. By calculating the Pearson correlation between acceleration data from inertial sensors and the positional data of specific points on the body, we aimed to determine whether the movements detected by the IMUs are accurately reflected in the kinematic displacements observed. This correlation analysis was performed for each kinematic dataset, focusing on key inertial points corresponding to relevant body segments.

The kinematic data were systematically grouped by body parts, such as lower limbs, upper limbs, and trunk; we conducted correlation analyses to understand how different body regions interacted with the inertial data. This systematic approach allowed us to identify which body parts and associated kinematic data most closely aligned with the inertial measurements and improved the visualization of the matrices.

The Pearson correlation analysis initially understood the linear relationships between the kinematic and inertial datasets. By computing the Pearson correlation coefficients for each pair of kinematic and inertial data points, we could identify instances where the inertial data closely matched the kinematic data. This step is essential in determining whether the IMUs could capture the same movement patterns as the more precise kinematic systems.

3.3.2 Cross-Correlation Analysis

Following the Pearson correlation analysis, we extended our investigation by applying a cross-correlation technique, which is particularly valuable for time series data as it measures the similarity between two signals over different time lags. This method shifts one signal relative to the other and calculates the correlation at each time shift, identifying the time lag that produces the highest correlation.

Even though the data were pre-aligned based on the collection time, cross-correlation provided a more refined analysis by determining the optimal temporal alignment between the inertial and kinematic signals. This precise alignment maximized the accuracy of the subsequent analyses, ensuring that the inertial data could be directly compared to the kinematic data at their most correlated time points.

We performed cross-correlation analyses for each combination of kinematic and inertial data points, systematically identifying which kinematic points exhibited the highest correlation with the inertial sensors. We established a threshold of 0.5 for the correlation coefficient, ensuring that only the most relevant and strongly correlated data points were considered. However, some kinematic points did not reach this threshold, indicating a weaker relationship with the inertial data. To address this, we implemented feature extraction techniques to enhance the correlation by deriving additional relevant metrics from the inertial data, thereby ensuring that all kinematic points had some degree of correspondence with the inertial measurements.

The combined use of Pearson correlation and cross-correlation provided an understanding of the relationships between kinematic and inertial data. These analyses demonstrated that, under the right conditions, inertial sensors could replicate kinematic data with high accuracy.

3.4 Features Extraction

We performed feature extraction from the inertial data to analyze correlations between inertial and kinematic data. In gait analysis, feature extraction from inertial data is crucial for establishing meaningful correlations with kinematic data. Inertial data from accelerometers and gyroscopes capture the forces and rotations acting on the body during movement. However, to make these data comparable and correlatable with kinematic data, which describe the actual movement of body segments, it is essential to extract and transform the raw information into features that reflect the dynamic and kinematic aspects of the movement.

These features facilitate the identification of movement patterns, enhancing our understanding of how forces and rotations influence body motion. Some extracted features include velocities (*vel*) along the X, Y, and Z axes. Velocity data, calculated by integrating acceleration data over time in each axis, is a fundamental feature that describes the translational movement of body segments. We obtained the angular acceleration (*ang_acc_gyro*) in the X, Y, and Z axes from the derivative of gyroscope data, which measures the rotation rate along the respective axes. This angular acceleration provides insights into how body parts rotate, which is essential for understanding the rotational movement of segments, such as the rotation of the trunk or limbs.

We obtained the magnitude of acceleration (*mag_acc*) from the square root of the sum of the squares of the accelerations along each of the three axes, representing the total intensity of the force acting on the body, yielding the total force associated with the movement. Similarly, the magnitude of angular velocity (*mag_gyro*) is calculated from the rotations measured by the gyroscopes. The harsh variation (*jerk*) along the X, Y, and Z axes, coming from the derivative of the acceleration, represents the acceleration rate change over time, providing information about abrupt modifications in the forces acting on the body.

Finally, position (*pos*) along the three axes was obtained by integrating the velocity data over time. This enabled us to estimate where the body segments are located in space, approaching a kinematic measure derived from velocity. Extracting these features from inertial data is relevant for identifying similarities between inertial and kinematic data and thus finding relationships in the IMU data that correspond to the behavior of all inertial points.

3.5 Clustering

After the correlation and cross-correlation analysis, it is crucial to evaluate whether the correlations observed between inertial and kinematic points can be verified using AI algorithms for pattern clustering and point correlation. Clustering after correlation analysis allows for identifying similar patterns, which is essential for better understanding the biomechanics of movement and differentiating subgroups of interest.

A new stage of data preparation is required to perform the clustering process. We based our approach on the correlation data between inertial and kinematic points with the highest Pearson and cross-correlation coefficients for a more accurate clustering process. We set a minimum correlation threshold of 0.5 between the inertial and kinematic points. Since the objective of this study is to assess whether kinematic data can be inferred from inertial data, the data were grouped so that for each kinematic point, all inertial data or features extracted from the inertial data were aggregated. Thus, all inertial data with a correlation greater than 0.5 were grouped for each kinematic point.

Next, the data needed to be resized for clustering using the K-Means algorithm. We experimented with two-dimensionality reduction techniques: Principal Component Analysis (PCA) and t-distributed Stochastic Neighbor Embedding (t-SNE). The choice of dimensionality reduction method is crucial for facilitating the visualization and interpretation of the formed clusters.

The data were transformed into a lower-dimensional space for each specified method, PCA or t-SNE. This step aims to reduce data complexity and improve clustering efficiency. We performed experiments using both methods, but PCA resulted in more tightly grouped and better-defined clusters. The number of clusters (n = 3) was selected based on criteria that balance the internal homogeneity of the clusters with the distinction between them. This selection was guided by the three phases of gait: left leg swing, stance, and right leg swing.

We evaluated the clusters using the Silhouette Score, Calinski-Harabasz Score, and Davies-Bouldin Index metrics that provide a quantitative view of cluster cohesion and separation, essential for validating the clustering results. After the initial clustering results, we proceeded to the step where the data were time-shifted according to the lag that yielded the best results in the cross-correlation analysis. With these adjustments, the clusters showed a significant improvement compared to the data without the time-shift adjustments related to the lag of the clusters.

3.6 Machine Learning

The next step in evaluating the similarities between kinematic and inertial data is assessing how well an ML algorithm can train a model and predict values in time series. To achieve this, we opted for an RF-based approach to predict kinematic gait variables, and complementary experiments were performed using Linear Regression for performance comparison.

The data follows from the conclusions drawn in the Pearson correlation and cross-correlation analysis stages, selecting values with a correlation modulus greater than 0.5, whether positive or negative, and using the time-shift adjustments. Cross-correlation data is helpful in assessing the temporal delay (lags) between IMU variables and the body points captured by the cameras.

The data was organized in a tabular format, where the input variables (X) are the IMU readings and the output variable (Y) is the coordinate of a specific body point. n inertial data points correspond to one kinematic value, as performed in the clustering experiment. The dataset was split into training and test sets, with 80% for training and 20% for testing.

We first implemented the RF algorithm, as state-of-the-art research indicates it performs well in training time series data related to gait. It is particularly effective with correlated and nonlinear variables. As a complementary evaluation, we implemented LR, which seeks to establish a linear relationship between the input, IMU, and output kinematic variables.

To assess the performance of the models, we calculated several metrics that are well-suited for time series analysis, including Mean Squared Error (MSE), which represents the average squared error between the predictions and actual values; R-Squared (R^2), indicating the proportion of variance explained by the model; Mean Absolute Error (MAE), which evaluates the average absolute error between predictions and actual values; Mean Absolute Percentage Error (MAPE), representing the average percentage error between predictions and actual values; and Relative Absolute Error (RAE), which compares the model's total absolute error to that of a simple baseline model.

We conducted an additional evaluation to understand which adjustments might be necessary to distribute IMU data during training for each kinematic point. We used the Feature Importance attribute from the RF model for this. Feature Importance helps identify the contribution of each feature in the training process, highlighting those with little relevance or detecting features that may introduce bias, leading to overfitting or poor model performance.

4 RESULTS AND DISCUSSION

This section encompasses three parts: the first focuses on the Pearson Correlation results (Section 4.1), in the sequence Cross-correlation (Section 4.2) results obtained, and the third Section 3.5 discusses and evaluates the clustering analysis's outcomes.

4.1 Pearson Correlation Analysis

The Pearson correlation analysis shows a strong match between the IMU and kinematic data in several instances, particularly regarding vertical foot movement and lateral trunk motion. This strong correlation suggests that wearables can accurately capture large displacements or rotations around specific axes, aligning closely with the patterns observed in the kinematic data. In some instances, however, the rotations detected by the IMUs correlate inversely with the movements seen in the kinematic data, indicating that the IMUs might be measuring rotations opposite to the linear motion. Nevertheless, more complex movements, such as accelerations along certain axes or specific rotations, show lower correlations, indicating limitations in the IMU sensors' ability to capture small-scale movements or intricate dynamic patterns.

One key finding is the high correlation between the Z-axis acceleration (*acc_z*) and the $c7_y$ point (located at the base of the neck), with a value of 0.6259 that indicates the vertical movement recorded by the accelerometer is strongly linked to the motion of the neck. When analyzing the foot and leg points (Figure 3), we see a higher correlation between the *gyro_x* and the $r\_knee\_1_y$ point (0.7616), suggesting that the gyroscope on the X-axis effectively captures the lateral motion of the right knee. Additionally, for the *gyro_z*-axis, there is a strong correlation with *l_knee_1_y* (0.6866), reinforcing the relationship between Z-axis rotations and knee movement.

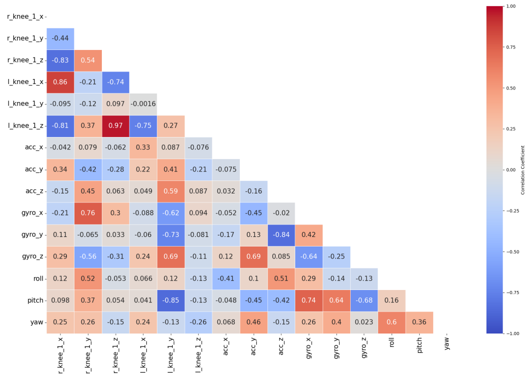

Figure 3: Correlation matrix of upper leg data against IMU.

The trunk points of Figure 4 show notable negative correlations between the *gyro_y*-axis and points such as *MIDASIS_y* (-0.6773), *r_asis_y* (-0.7107), and *l_asis_y* (-0.5705), suggesting the Y-axis rotation could be related to an opposite or compensatory movement in the pelvis and waist points. Regarding force plates, correlations between *gyro_x* and *r_force_x* (-0.5781) and *r_force_y* (-0.5133) indicate that the gyroscopes may capture the impact or force exerted on the right leg during motion.

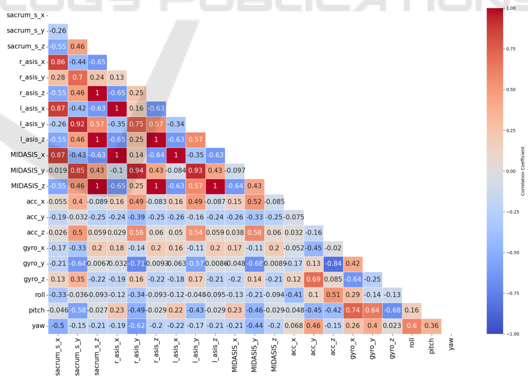

Figure 4: Correlation matrix of trunk data against IMU.

In terms of velocity and displacement, the linear velocities along the X-axis (*vel_x*) stand out with extremely high correlations (close to 1.0) with several body points, such as *c7_z*, *SHO_z*, and *MIDASIS_z*, among others in both the upper and lower body, suggesting coordinated and consistent movement in a specific direction during gait.

The most significant correlations in the analyzed groups exceed 0.5, highlighting the IMU's ability to capture movements related to kinematic points, mainly vertical and rotational.

When the correlation threshold is lowered to 0.4, more moderate correlations emerge, especially in horizontal movements and regions that are harder to measure precisely, such as lateral movements of the trunk and head. Despite this, most correlations remain above this threshold, supporting that IMUs can extract useful information for analysis similar to kinematic data across multiple dimensions.

The fact that most correlations are above 0.5 or 0.4 suggests that the IMU sensors capture movement accurately compared to kinematic points, particularly regarding vertical and rotational movements. However, there are limitations in lateral movements and specific acceleration axes, where correlations tend to be lower.

4.2 Cross-Correlation Analysis

These cross-correlation data highlight the relationships between inertial device variables and kinematic variables of anatomical reference points. Cross-correlation measures how two-time series shift relative to each other, while lag represents the time difference between the two signals that maximizes this correlation. This step is essential to align the data and optimize their correlation.

For instance, the X-axis acceleration from the accelerometer is strongly correlated with the vertical displacement of the *r_asis_y* (Figure 5), hip region, with a lag of 34 samples. Similarly, the Z-axis rotation from the gyroscope is highly correlated with the Y-axis force of the right leg's force point, showing a lag of 72 samples, suggesting a relatively strong synchronization.

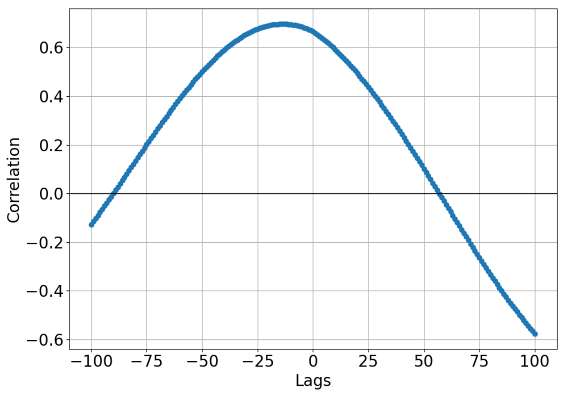

Figure 5: Cross-correlation matrix of trunk data against IMU.

The Z-axis acceleration is closely correlated with the vertical movement of the C7 point located at the upper back, indicating synchronized vertical motions between the trunk and the vertical acceleration measured by the device. Some variables display significant negative correlations, which could indicate opposing movements or inverse relationships between the forces/movements captured by the sensors. For example, the Y-axis accelerometer (*acc_y*) and the right heel Y-axis position (*r_heel_y*) have a correlation of -0.82 (Figure 6), suggesting that as Y-axis acceleration increases, the right heel's vertical position decreases. Similarly, the *gyro_y*-axis rotation and the sacrum Y-axis position (*sacrum_s_y*) have a negative correlation of -0.77.

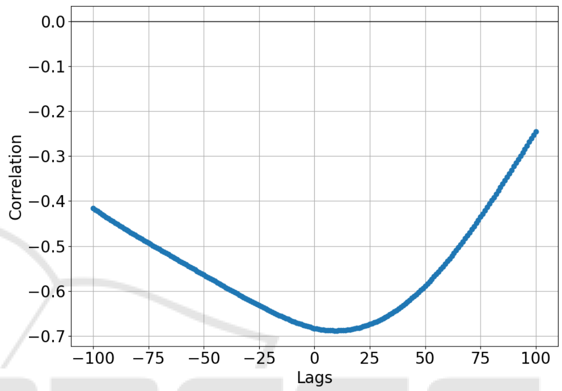

Figure 6: Cross-correlation matrix of trunk data against IMU.

The analysis shows strong correlations between IMU and kinematic data for several variables, with some correlations being exceptionally high (above 0.8). However, there is a need for temporal alignment (lag) to improve the precision of the match between the two data types. Additionally, it is crucial to consider that some variables have negative correlations, suggesting a more complex dynamic in the movement. These findings indicate that, with adjustments in lag and a deeper analysis of inversely correlated variables, it is possible to achieve effective integration between IMU and kinematic data to describe movement accurately.

4.3 Clustering Analysis

Based on the clustering data involving IMU variables and kinematic points, we analyzed kinematic and inertial data. We grouped the inertial points that exhibited the highest correlation with each kinematic point, taking into account the most appropriate lag for each relationship. The metrics used to evaluate the clusters were the Silhouette Score, Calinski-Harabasz Score, and Davies-Bouldin Index. When graphically analyzing the clusters, we observe the variables along the axes as Principal Component 1 and Principal Component 2. These represent the two dimensions of the data transformed through PCA, capturing the most significant variations. Principal Component 1 accounts for the direction of maximum variance, while Principal Component 2 captures the second most significant variance in the data.

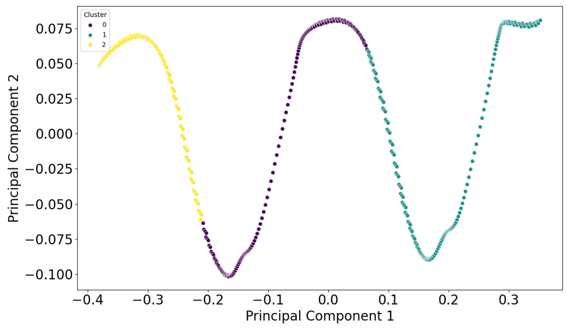

Figure 7: Clustering using K-Means for 3 clusters with PCA and adjustment of inertial data according to the best lag. The left ankle *l_mall* point on the Z-axis and inertial data with the best correlation.

The Silhouette Score (SS), which ranges from -1 to 1, measures how well a data point is associated with its cluster compared to others. Figure 7 displays that most variable pairs achieved SS values around 0.5 to 0.65, indicating that the clusters are reasonably well-formed. Scores above 0.6 are considered good, while those below 0.4 may suggest an overlap between clusters.

The Calinski-Harabasz metric measures dispersion within and between clusters; a higher score indicates better separation between clusters. Figure 8 shows that the variables related to the X-axis of the left knee (*l_knee*) and the left metatarsal (*l_met_x*) stood out with scores above 5000, indicating excellent separation between these clusters. Conversely, pairs like the right metatarsal on the X-axis and sacrum on the Y-axis displayed lower scores below 1500, suggesting poor separation.

The Davies-Bouldin Index evaluates the similarity rate between clusters. Unlike the other metrics, a lower value indicates that the clusters are more compact and well-separated. We observed higher indices for variables such as *r_asis_y* and *MIDASIS_y*, suggesting that these clusters may be poorly defined or exhibit significant overlap. In contrast, variables like *l_mall_z* and *l_heel_z* showed low values, indicating that these clusters are compact and distinct.

An analysis of the X and Z axes, such as C7 on the X-axis, the right shoulder on the Z-axis, and the left mall on the Z-axis, revealed higher Silhouette Scores (> 0.55) and lower Davies-Bouldin Index values (0.5–0.7) (Figure 9, suggesting that the clusters associated with these axes are well-defined. We can conclude that movements or displacements along these axes are more easily distinguishable by the clusters, particularly in segments like the knee and metatarsal.

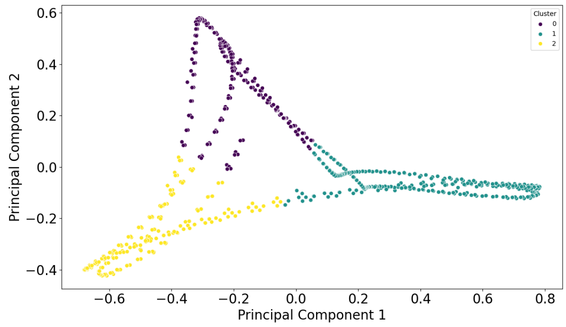

Figure 8: Clustering using K-Means for 3 clusters with PCA and adjustment of inertial data according to the best lag. The left knee *l_knee* point on the X-axis and inertial data with the best correlation.

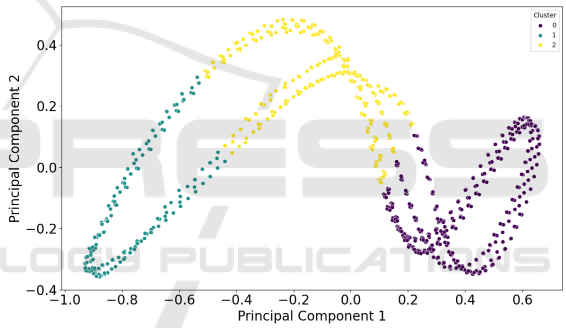

Figure 9: Clustering using K-Means for 3 clusters with PCA and adjustment of inertial data according to the best lag. The center of mass *SHO* point on the X-axis and inertial data with the best correlation.

Concerning the Y-axis, such as *c7_y*, *r_should_y*, *MIDASIS_y*, the Silhouette Scores were relatively low (around 0.35–0.4), while the Davies-Bouldin Index values were higher (0.9). These findings suggest that the clusters along the Y-axis may not be as well-defined, possibly due to the complexity of vertical movement during gait, which tends to be more continuous with fewer abrupt changes. For the Y-axis, conducting additional experiments and seeking complementary approaches to improve the data quality will be necessary.

Variables such as *l_knee_1_z* and *l_mall_z* exhibited high Calinski-Harabasz Scores and low Davies-Bouldin Index values, indicating that the movements of the knees and ankles, particularly in the sagittal plane, are well-separated in clusters, reflecting the importance of these joints in propulsion and phase transitions during gait. Regarding central points like the sacrum on the Z-axis (*sacrum_s_z*) and the midpoint between the point of the iliac crest on the X-axis (*MIDASIS_x*), we observed a combination of favorable results, with Silhouette Scores above 0.6 and low Davies-Bouldin Index values, indicating that the clusters for these central body points are well-separated.

The variables *l_mall_z*, *l_knee_1_z*, *l_met_x*, and *MIDASIS_x* demonstrated an excellent combination of clustering metrics, meaning that they are well-suited to describe different phases of gait or variations in movement. However, variables associated with the Y-axis, such as *r_asis_y*, *r_met_x*, and *MIDASIS_y*, indicate that the clusters are not well-defined, suggesting that the data or movements captured along these axes do not vary significantly between phases or subjects or that substantial overlap exists.

4.4 Machine Learning Analysis

The evaluation metrics reveal that using IMU data, the Random Forest (RF) model performed robustly in predicting gait kinematic points. Most kinematic points, such as *c7_z*, *r_should_z*, *l_should_z*, *sacrum_s_z*, and *r_mall_z*, showed low MSE, around 10^{-7}, indicating high accuracy in predictions. When assessing R^2 values, we observed results close to 1, as 0.99996 for *c7_z*, suggesting the model captures almost all the variance, providing a good fit for these parameters. However, some points like *l_met_y* (R-Squared of 0.995) and *r_met_y* (R^2 of 0.997) showed a lower performance in terms of variance explanation, suggesting the model may struggle with these specific cases. Still, these values remain above 0.99, which overall represents strong performance.

We observed low MAE values, such as the right shoulder on the Z-axis (*r_should_z*) with 0.00045, indicating that the predictions are very close to the actual values in measurement units. The MAPE for most points is extremely low, such as 0.0011% for *c7_z*. However, points like *MIDASIS_y* (MAPE of 10%) and *r_met_y* (MAPE of 5%) showed higher errors, indicating that the model has more difficulty accurately predicting these points, likely due to the increased complexity of the Y-axis data.

The data suggests the model performs consistently across predictions in the X, Y, and Z directions, with larger errors occurring along the Y-axis, such as in left heel (*l_heel_y*) and left metatarsal (*r_met_y*), which may be attributed to greater variability in human movement along this axis, associated with vertical motion during gait. Comparing the LR results with those of RF, we observe that RF has superior overall performance regarding data fit (R-Squared) and prediction accuracy (MSE, MAE, RAE, MAPE), especially for more complex variables. Linear Regression performs reasonably but with more significant variation in results and higher errors for many variables, suggesting it does not capture the non-linearity present in gait data as effectively.

Considering the feature importance in the RF model, we found that for many points, such as *c7_x*, *r_should_x* (Figure 10), *sacrum_s_x*, and *l_asis_x*, speed along the X-axis (*vel_x*) plays a significant role compared to other variables, with velocity along this axis being a strong predictor in the model. Velocity along the Z-axis is also relevant, particularly for points like *c7_x*, *r_should_z*, and *sacrum_s_z*.

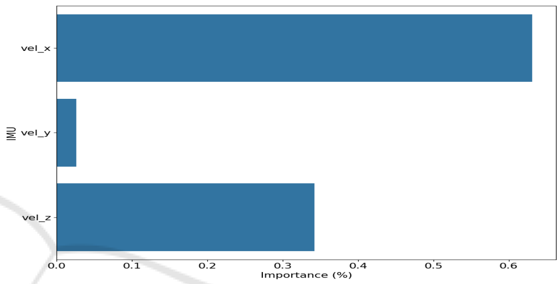

Figure 10: Feature importance of IMU data in training the right shoulder X-axis model.

Speed along the Y-axis (*vel_y*) shows variable importance, often lower than the X and Z axes, indicating that lateral velocity may be less crucial to the overall gait behavior. Variables related to acceleration (*acc_x*, *acc_z*) and position (*pos_x*, *pos_z*) show significant importance, such as in *c7_y*, *r_should_y*, and *MIDASIS_y* (Figure 11), suggesting that these variables may be linked to critical gait events, like direction changes or acceleration/deceleration.

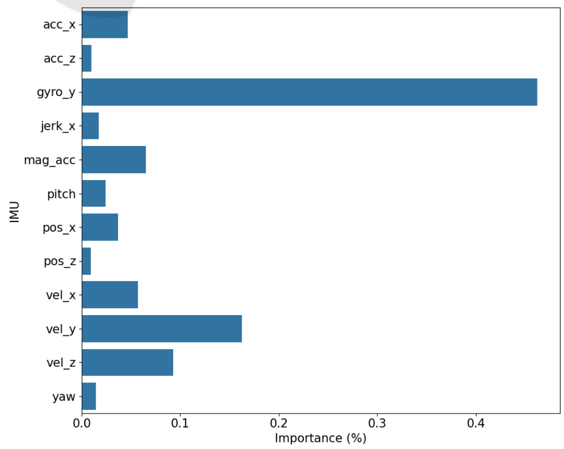

Figure 11: Feature importance of IMU data in training the model for the midpoint between the iliac crests on the Y-axis.

Yaw shows relevant importance for specific points, such as *r_should_y* (Figure 12), *l_should_x*, and *r_asis_y*, indicating that rotational movement around the vertical axis is significant for predicting kinematic data. Roll and pitch exhibit relatively lower importance, suggesting that while they influence gait, they are less critical in determining the overall movement.

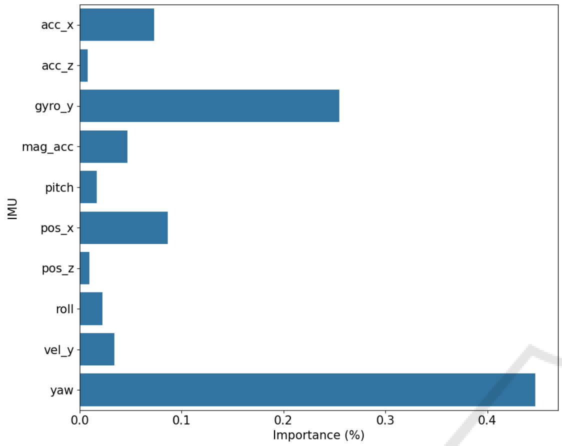

Figure 12: Feature importance of IMU data in training the model for the right shoulder on the Y-axis.

5 CONCLUSION

This study evaluated the similarity between signals from biomechanics laboratories, considered the gold standard in gait analysis, and inertial data from wearable devices, which are more accessible and cost-effective. Achieving the same mathematical results from different gait analysis instruments would represent a significant breakthrough in the field. To assess the correspondence between the two datasets, some experiments were conducted, comprising data collection followed by preprocessing and various mathematical analyses, including artificial intelligence models to predict kinematic points based on sensor data.

Pearson correlation analysis presented promising results with good correspondence between IMU sensor data and kinematic data, particularly in vertical movements and rotations along specific axes. Anatomical points, such as the base of the neck (C7) and the right knee, exhibited strong correlations, suggesting that inertial sensors can reliably capture key movements. However, accelerations on the y-axis and lateral motions showed lower correlations, revealing a limitation of the IMU sensors in detecting small displacements or intricate movements. Additionally, some negative correlations suggest that the sensors may be capturing rotations or movements opposite to expectations, which could reflect natural compensations in the body during gait–an important factor that may not necessarily be a flaw but should be considered.

Cross-correlation analysis emphasized the need for temporal alignment between inertial and kinematic data. The significant time lags observed between some variables indicate delays that should be corrected to improve the accuracy of the correlations. Clustering analysis revealed that movements along the X and Z axes, especially around the knee and ankle joints, are well-defined and show clear separation between clusters. However, clustering movements along the Y-axis posed challenges, with low scores on the Silhouette and Davies-Bouldin indices indicating difficulties distinguishing these movements.

Improving the temporal alignment between IMU and kinematic data is essential. Lateral movements and specific accelerations also require more attention, suggesting the need for new experiments or more sensitive sensors. Despite these challenges, the positive results indicate that using inertial sensors remains a promising avenue, particularly for capturing large displacements and rotations, with great potential for integration into more gait analysis systems.

The RF model performed excellently in predicting kinematic points based on sensor data, with low error rates and high R-Squared values for most points. A few points with higher MAPE and RAE could benefit from further refinement, potentially through model architecture or input data adjustments. The RF approach appears effective and well-suited for predicting kinematic gait data.

For future work, it is essential to focus on improving the data related to the Y-axis and refining the clustering across all anatomical points. Additionally, the application of Machine Learning algorithms for time series analysis holds promise, enabling more accurate predictions and automatic pattern detection in gait. As these techniques evolve, the accuracy and utility of inertial data will be expected to improve, making wearables increasingly effective tools for gait analysis in clinical and athletic settings.

REFERENCES

Akhtaruzzaman, M., Shafie, A., and Khan, M. (2016). Gait analysis: Systems, technologies, and importance. *Journal of Mechanics in Medicine and Biology*, 16(07):1630003.

Benson, L., Clermont, C., Bošnjak, E., and Ferber, R. (2018). The use of wearable devices for walking and running gait analysis outside of the lab: A systematic review. *Gait and Posture*, 63:124–138.

Borzì, L., Sigcha, L., Rodríguez-Martín, D., and Olmo, G. (2023). Real-time detection of freezing of gait in parkinson's disease using multi-head convolutional neural networks and a single inertial sensor. *Artificial Intelligence in Medicine*, 135:102459.

BTS Bioengineering (2024a). BTS G-WALK - Wireless Sensor for Gait Analysis. https://www.btsbioengineering.com/products/g-walk/. Accessed: 2024-08-31.

BTS Bioengineering (2024b). BTS GAITLAB - 3D Motion Analysis System. https://www.btsbioengineering.com/products/bts-gaitlab/. Accessed: 2024-08-31.

Burdack, J., Horst, F., Giesselbach, S., Hassan, I., Daffner, S., and Schöllhorn, W. I. (2020). Systematic comparison of the influence of different data preprocessing methods on the performance of gait classifications using machine learning. *Frontiers in Bioengineering and Biotechnology*, 8.

Caldas, R., Sarai, R., Buarque de Lima Neto, F., and Markert, B. (2020). Validation of two hybrid approaches for clustering age-related groups based on gait kinematics data. *Medical Engineering & Physics*, 78:90–97.

da Rosa Tavares, J., Ullrich, M., Roth, N., Kluge, F., Eskofier, B., Gaßner, H., Klucken, J., Gladow, T., Marxreiter, F., da Costa, C., da Rosa Righi, R., and Victória Barbosa, J. (2023). utug: An unsupervised timed up and go test for parkinson's disease. *Biomedical Signal Processing and Control*, 81:104394.

Delval, A., Betrouni, N., Tard, C., Devos, D., Dujardin, K., Defebvre, L., Labidi, J., and Moreau, C. (2021). Do kinematic gait parameters help to discriminate between fallers and non-fallers with parkinson's disease? *Clinical Neurophysiology*, 132(2):536–541.

Desai, R., Martelli, D., Alomar, J., Agrawal, S., Quinn, L., and Bishop, L. (2024). Validity and reliability of inertial measurement units for gait assessment within a post stroke population. *Topics in Stroke Rehabilitation*, 31(3):235–243. PMID: 37545107.

He, Y., Chen, Y., Tang, L., Chen, J., Tang, J., Yang, X., Su, S., Zhao, C., and Xiao, N. (2024). Accuracy validation of a wearable imu-based gait analysis in healthy female. *BMC Sports Science, Medicine and Rehabilitation*, 16(1):2.

Jakob, V., Küderle, A., Kluge, F., Klucken, J., Eskofier, B., Winkler, J., Winterholler, M., and Gassner, H. (2021). Validation of a sensor-based gait analysis system with a gold-standard motion capture system in patients with parkinson's disease. *Sensors*, 21(22).

Kim, H., Kim, Y.-H., Kim, S.-J., and Choi, M.-T. (2022). Pathological gait clustering in post-stroke patients using motion capture data. *Gait & Posture*, 94:210–216.

Kotiadis, D., Hermens, H., and Veltink, P. (2010). Inertial gait phase detection for control of a drop foot stimulator: Inertial sensing for gait phase detection. *Medical Engineering and Physics*, 32(4):287–297.

Kvist, A., Tinmark, F., Bezuidenhout, L., Reimeringer, M., Conradsson, D., and Franzén, E. (2024). Validation of algorithms for calculating spatiotemporal gait parameters during continuous turning using lumbar and foot mounted inertial measurement units. *Journal of Biomechanics*, 162:111907.

Millecamps, A., Lowry, K., Brach, J., Perera, S., Redfern, M., and Sejdić, E. (2015). Understanding the effects of pre-processing on extracted signal features from gait accelerometry signals. *Computers in Biology and Medicine*, 62:164–174.

Nguyen, A., Roth, N., Ghassemi, N., Hannink, J., Seel, T., Klucken, J., Gassner, H., and Eskofier, B. (2019). Development and clinical validation of inertial sensor-based gait-clustering methods in parkinson's disease. *Journal of NeuroEngineering and Rehabilitation*, 16(1):77.

Parashar, A., Parashar, A., Ding, W., Shabaz, M., and Rida, I. (2023). Data preprocessing and feature selection techniques in gait recognition: A comparative study of machine learning and deep learning approaches. *Pattern Recognition Letters*, 172:65–73.

Ripic, Z., Nienhuis, M., Signorile, J., Best, T., Jacobs, K., and Eltoukhy, M. (2023). A comparison of three-dimensional kinematics between markerless and marker-based motion capture in overground gait. *Journal of Biomechanics*, 159:111793.

Rousanoglou, E., Foskolou, A., Emmanouil, A., and Boudolos, K. (2024). Inertial sensing of the abdominal wall kinematics during diaphragmatic breathing in head standing. *Biomechanics*, 4(1):63–83.

Silva, L. and Stergiou, N. (2020). Chapter 7 - the basics of gait analysis. In Stergiou, N., editor, *Biomechanics and Gait Analysis*, pages 225–250. Academic Press.

Tsakanikas, V., Ntanis, A., Rigas, G., Androutsos, C., Boucharas, D., Tachos, N., Skaramagkas, V., Chatzaki, C., Kefalopoulou, Z., Tsiknakis, M., and Fotiadis, D. (2023). Evaluating gait impairment in parkinson's disease from instrumented insole and imu sensor data. *Sensors*, 23(8).

Zhang, Y., Wang, M., Awrejcewicz, J., Fekete, G., Ren, F., and Gu, Y. (2017). Using gold-standard gait analysis methods to assess experience effects on lower-limb mechanics during moderate high-heeled jogging and running. *Journal of visualized experiments : JoVE*, 127:55714.

Zhou, L., Tunca, C., Fischer, E., Brahms, C., Ersoy, C., Granacher, U., and Arnrich, B. (2020). Validation of an imu gait analysis algorithm for gait monitoring in daily life situations. In *Annual International Conference of the IEEE Engineering in Medicine and Biology Society (EMBC)*, pages 4229–4232.